

Surface roughening during low-temperature Si epitaxial growth on singular vs vicinal Si(001) substrates

N.-E. Lee, David G. Cahill, and J. E. Greene

Materials Science Department, the Coordinated Science Laboratory, and the Materials Research Laboratory, University of Illinois, 1101 West Springfield Avenue, Urbana, Illinois 61801

(Received 25 August 1995)

The evolution of surface roughness on epitaxial Si films grown at 300 °C by ultrahigh vacuum ion-beam sputter deposition onto nominally singular, [100]-, and [110]-miscut Si(001) is inconsistent with conventional scaling and hyperscaling laws for kinetic roughening. Unstable growth leading to the formation of mounds separated by a well-defined length scale is observed on all substrates. Contrary to previous high-temperature growth results, the presence of steps during deposition at 300 °C increases the tendency toward unstable growth resulting in a much earlier development of mound structures and larger surface roughness on vicinal substrates.

I. INTRODUCTION

The dynamics of surface morphological evolution during film growth from the vapor phase have been of increasing technological and scientific interest over the last several years. Thin-film applications demand ever lower growth temperatures in order to, for example, obtain abrupt interfaces in multilayer devices, minimize alloy and dopant interlayer diffusion, and inhibit phase transitions in metastable materials. However, low-temperature growth has generally been found to lead to surface roughening. This, in turn, has sparked intensive theoretical investigation of kinetic roughening during epitaxial growth. Much of this work has been based on the assumption that roughening can be modeled using scaling theory applied to growth surfaces which exhibit self-affine characteristics. Under this hypothesis, roughness evolves with a temporal and scale-invariant structure.¹⁻³ While many experiments on surface roughening during film growth have been interpreted in the context of the dynamic scaling hypothesis, no consensus has emerged concerning the relationship between roughness and growth exponents appropriate to a given growth process.¹⁻¹⁰

Villain⁴ pointed out the potential importance of diffusion bias in influencing the evolution of surface roughness. The term refers to the fact that the adatom diffusion current on a vicinal surface is not zero if there is an asymmetry in the attachment probabilities at ascending and descending steps. Such an asymmetry has been shown by Ehrlich and co-workers, using field ion microscopy, to exist on W(111) (Ref. 11) and Ir(111) (Ref. 12) surfaces in the form of barriers to adatoms crossing over descending steps and trapping sites for terrace adatoms approaching ascending steps. The experimental evidence for ascending/descending step attachment asymmetry is not as clear for surfaces on diamond-structure semiconductors. However, differences in adatom sticking probabilities at *A* and *B* steps on Si(001) have been observed by scanning tunneling microscopy.¹³ Moreover, computer simulations show that there is a much larger activation energy for adatoms diffusing to descending *A* steps than to descending *B* steps,^{14,15} and total-energy calculations predict that while there is a strong reflecting barrier at descending *A* steps, the barrier at descending *B* steps is much smaller.¹⁶

The presence of a diffusion bias during growth in the step-flow mode is predicted to stabilize smooth growth surfaces due to a substrate-tilt-dependent diffusion current, while terrace nucleation destabilizes the growth surface by reducing the current and leading to layer-by-layer growth with the production of moundlike or pyramidlike structures.⁶⁻⁹ Such growth mounds have been reported during the elevated-temperature layer-by-layer molecular-beam epitaxial (MBE) growth of GaAs on near-singular GaAs(001) substrates, but were not observed during deposition on vicinal substrates where the presence of additional steps inhibited nucleation on the terraces and resulted in step-flow growth with smooth surfaces.⁷ In this case, steps stabilized the growth surface.

Instabilities leading to the formation of mounds have also been reported during low-temperature MBE of Cu (Ref. 17) and Ge (Ref. 18) in the two-dimensional (2D) multilayer¹⁹ growth mode on near-singular (001) substrates. However, the role of steps in influencing the evolution of surface roughening in this growth mode, where high terrace nucleation rates minimize substrate-tilt-induced diffusion currents, has not been addressed. In this paper, we show, using atomic force microscopy (AFM), that, surprisingly, and contrary to the high-temperature step-flow case, the use of vicinal substrates during low-temperature epitaxy of Si(001) enhances growth instabilities leading to earlier development of growth mound structures and larger surface roughnesses. The films were grown from hyperthermal Si beams (average energy/particle ≈ 18 eV) provided by ultrahigh-vacuum (UHV) Kr⁺-ion-beam sputtering. The technique was chosen since it was previously shown to yield critical epitaxial Si thicknesses which are approximately an order of magnitude larger than those obtainable by MBE over the same temperature range,²⁰ thus allowing roughness measurements to be carried out over a much wider range of layer thicknesses.

II. EXPERIMENTAL PROCEDURE

All film growth experiments were conducted in a three-chamber load-locked 1×10^{-10} -Torr UHV system with facilities for reflection high-energy electron diffraction (RHEED), residual gas analysis, and Auger-electron spectroscopy (AES).^{20,21} Sputtering was carried out using an

UHV double-grid multiaperture broad ion-beam source with the extracted beam focused by a postextraction unipotential electrostatic ion lens. High-purity energetic Si beams, with average Si-atom energies of 18 eV, were generated by bombarding an undoped 10-cm-diameter float-zone Si(001) wafer using a 1-keV ultrahigh-purity Kr⁺ ion beam.^{20,21} The design of the system geometry together with the use of higher mass Kr⁺ ions, rather than Ar⁺, minimized energy transfer to the growth surface from backscattered ions.²⁰ Incorporated metallic impurity concentrations were below secondary-ion-mass-spectrometry detection limits ($\approx 1 \times 10^{15} - 10^{16} \text{ cm}^{-3}$).²¹

The primary substrates used in these experiments were Si(001)2×1 wafers either nominally singular, with miscuts as measured by high-resolution x-ray diffraction of 0.16° toward [110] corresponding to an average terrace width l of 50 nm, or vicinal with miscuts of 4° toward [100] ($l=2$ nm). The Si(001)-4° [100] surface consists of terraces bounded by single-atom height steps composed of equal fractions of A and B edges. A few 4°[110] miscut ($l=2$ nm) samples were also examined for comparison. Substrate preparation consisted of degreasing followed by a UV ozone treatment,^{20,21} H passivation in dilute HF, degassing in UHV at 200 °C for 1 h, oxide desorption at 700 °C for 10 s, and the growth of 100-nm-thick Si buffer layers. Buffer layer growth temperatures were chosen to be 650 and 600 °C on singular and vicinal substrates, respectively, in order to obtain comparably smooth starting surfaces with nearly equal short-range roughnesses as judged by correlated height-difference measurements (see Fig. 2 below). RHEED patterns were 2×1 with sharp Kikuchi lines, and no residual C or O was detected by AES. AFM measurements were carried out in air using a Digital Instruments Nanoscope II with oxide-sharpened Si₃N₄ tips whose radii were 5–40 nm. TEM and cross-section transmission electron microscopy (XTEM) analyses were performed using Philips CM-12 and Hitachi 9000 microscopes operated at 120 and 300 kV, respectively.

III. RESULTS AND DISCUSSION

All films used in this investigation were single crystals of high structural quality with no defects observable by conventional or high-resolution TEM and XTEM. That is, film thicknesses were always less than critical epitaxial values t_{epi} which were found to be 1200 nm for growth on singular Si(001) at $T_s=300$ °C,²⁰ and ≈ 800 and 500 nm, respectively, on the [100]- and [110]-miscut substrates.

Some typical AFM images of the surfaces of Si films grown to different nominal layer thicknesses t on singular and vicinal Si(001) substrates are presented in Fig. 1. The surface morphology of 50-nm-thick layers (not shown) grown on singular substrate is relatively flat with no detectable features. Further growth, however, leads to the development of features, linearly anisotropic along $[\bar{1}10]$ [see, for example, Fig. 1(a) corresponding to $t=500$ nm]. Compact well-defined growth mounds are clearly observed on singular substrates at $t=800$ nm [Fig. 1(b)]. In contrast, the initiation of mound formation is already evident at $t=50$ nm (not shown) on the [100]-miscut vicinal surface and the mounds continuously coarsen with further deposition as shown in Figs. 1(c) ($t=200$ nm) and 1(d) ($t=500$ nm). The behavior

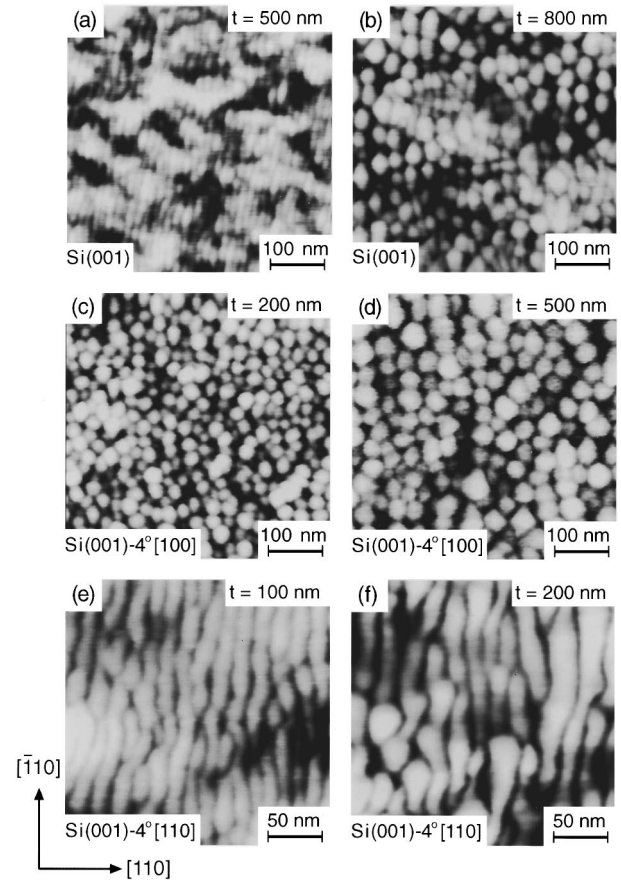


FIG. 1. AFM images of the surfaces of epitaxial Si films grown on Si(001) substrates at $T_s=300$ °C. Substrate miscut direction, film thicknesses, and the black-to-white gray scales are (a) singular, 500 and 4 nm; (b) singular, 800 and 8 nm; (c) [100], 200 and 3 nm; (d) [100], 500 and 4 nm; (e) [110], 100 and 7 nm; and (f) [110], 200 and 7 nm.

on the [110]-miscut surface is similar to that of the [100]-miscut surface, except that the mounds exhibit a strong shape anisotropy along the initial $[\bar{1}10]$ step direction as shown in Figs. 1(e) and 1(f).

In all cases, the growth mounds we observe are compact objects rather than fractal in nature, and thus are not expected to obey conventional scaling models for kinetic surface roughening. Nevertheless, the height difference correlation function $G(\rho, t) = \langle [h(j, t) - h(i, t)]^2 \rangle$, where ρ is the separation of positions i and j , still provides a quantitative measure of the evolution of surface roughness. Analyses of AFM data for films with thicknesses t between 50 and 1000 nm on singular surfaces and 50 and 500 nm on [100]-miscut surfaces were carried out. The results are presented in Figs. 2(a) and 2(b) as the root-mean-correlated height difference $[G(\rho, t)]^{1/2}$ vs ρ in a log-log plot. With the exception of the data for $t \leq 50$ nm on singular substrates for which no growth mounds were observed, the two sets of curves exhibit similar behavior. G increases with ρ following a power-law behavior until saturation is reached for each film thickness. Note that, contrary to the predictions of conventional kinetic roughening models assuming self-affine surfaces,^{3,22} $G(\rho, t)$ increases with increasing t at a given value of ρ in the pre-saturation region.

Effective roughening and growth exponents α and β were

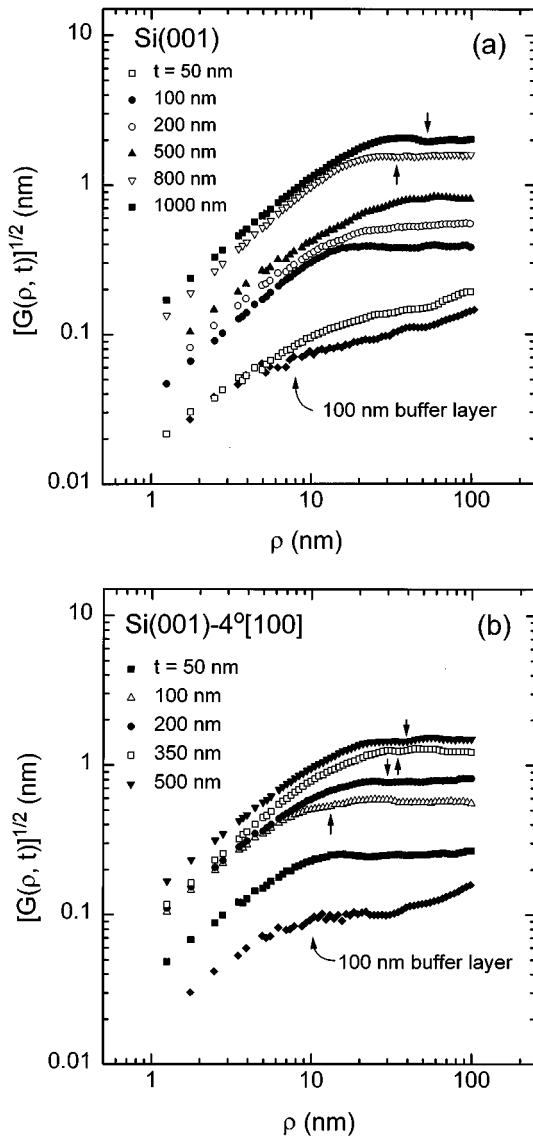


FIG. 2. Root-mean-correlated height difference $[G(\rho, t)]^{1/2}$ vs the separation ρ of positions i and j on the surfaces of epitaxial Si films grown at 300°C to thicknesses $t=50\text{--}1000$ nm on (a) nominally singular and (b) 4° [100]-miscut substrates. Arrows mark the average separation between growth features. For comparison, data from high-temperature buffer layers are included.

determined from the data in Fig. 2 using the scaling relationships $G(\rho, t) \propto \rho^{2\alpha}$ for small ρ and $G(\rho, t) \propto t^{2\beta}$ for $\rho \rightarrow \infty$. Physically, α is a measure of how well the roughness can be described by a single lateral length scale (e.g., a periodic surface roughness corresponds to $\alpha=1$), while β is a measure of how fast the roughness develops.²² In Fig. 2, $\alpha_{\text{eff}}=0.85 \pm 0.05$ for growth with $t=200\text{--}1000$ nm on singular surface and 0.80 ± 0.05 for growth with $t=50\text{--}500$ nm on [100]-miscut surfaces,²³ both remarkably similar to the value obtained for low-temperature MBE Ge growth on Ge(001), 0.80 ± 0.05 .¹⁸ $[G(\infty, t)]^{1/2}$ is plotted vs film thickness in Fig. 3, from which we extract a value of $\beta_{\text{eff}}=0.7 \pm 0.05$ for growth in the saturation range ($t=100\text{--}500$ nm) on [100]-miscut substrates. For growth on singular substrates, $\beta_{\text{eff}}=0.6 \pm 0.05$ over the same film thickness range followed by a rapid increase in β_{eff} to values

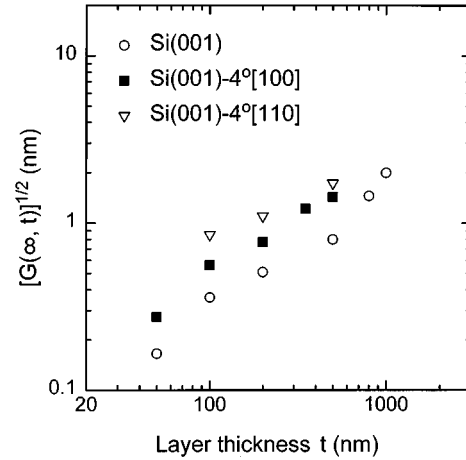


FIG. 3. Saturated root-mean-correlated height difference $[G(\rho \rightarrow \infty, t)]^{1/2}$ vs film thickness for epitaxial Si films grown at $T_s=300^\circ\text{C}$ on nominally singular Si(001), Si(001)- 4° [100], and Si(001)- 4° [110] substrates. $[G(\rho \rightarrow \infty, t)]^{1/2}$ is defined here as the average of all measured G values obtained for ρ larger than that corresponding to the intersection of best-fit straight lines drawn through the steeply rising and saturation regions of $[G(\rho, t)]^{1/2}$ vs ρ data in Fig. 2.

>1 for $t > 500$ nm. α_{eff} and β_{eff} values for [110]-miscut samples were found to be similar to those of the [100]-miscut sample with slightly larger $[G(\infty, t)]^{1/2}$ values, as shown in Fig. 3. The exponents obtained from our measurements are all larger than those predicted by scaling theories for the ballistic aggregation “hit and stick” ($\alpha=\frac{1}{3}, \beta=\frac{1}{3}$).² They also do not agree with the hyperscaling relationship $2\alpha=(\alpha/\beta-2)$,⁵ derived for deposition under conditions in which deposited adatoms are allowed to relax by surface diffusion into positions of higher bonding coordination.

The temporal evolution of the lateral spread of surface height fluctuations can be characterized by the average mound separation obtained from the first maximum in the height-height correlation function $\langle h(i, t)h(j, t) \rangle$, or the first weak local minimum in $[G(\rho, t)]^{1/2}$ vs ρ curves, as indicated, for example, by arrows in Fig. 2(b). The average mound separation d ranged from $\approx 34\text{--}48$ nm for film thicknesses between 800 and 1000 nm on singular substrates and $\approx 14\text{--}40$ nm for $t=100\text{--}500$ nm on [100]-miscut substrates, consistent with the finding that during growth in the 2D multilayer mode, the mounds coarsen much faster on vicinal than on singular surfaces. The relationship between d and t for growth on [100]-miscut substrates followed a power-law dependence, $d \propto t^\gamma$, where $\gamma \approx 0.7$.

The instability giving rise to the development of the observed growth mounds separated by a well-defined length scale cannot be explained simply by statistical fluctuations in the growth flux.^{18,24} This is easily demonstrated using the simple model presented in Refs. 4 and 18 to estimate the magnitude of height fluctuations due to noise combined with surface smoothing by diffusion. Root-mean-square surface roughness values obtained for a 500-nm-thick film grown on a [100]-miscut substrate are approximately a factor of 30 smaller than our measured values. Moreover, the use of vicinal substrates, in which the average terrace width is of the order of adatom mean free paths (estimated, based upon data

in Ref. 13, to be 2–3 nm at 300 °C), would be expected to lead toward stable step-flow growth rather than to the growth instabilities we observe.

We propose that the primary source of the growth instability during low-temperature deposition on singular and miscut Si(001) surfaces stems from the anisotropy in diffusion along and across dimer rows¹³ combined with adatom trapping near descending A-step edges,¹⁴ leading to enhanced extrinsic island nucleation. In the case of miscut substrates, where the step density is high, we expect that extrinsic island nucleation rates will far exceed the rate of intrinsic random terrace nucleation, resulting in a larger roughness and a much earlier development of growth mounds. This tendency is consistent with both our AFM images and the results in Fig. 2, showing that the absolute values of the root-mean height-difference correlation functions were large, at comparable film thicknesses, on the vicinal surfaces. An increase in the rate of surface roughening is also expected to result in reduced critical epitaxial thicknesses, in agreement with our experimental observations in which t_{epi} (300 °C) decreases from 1200 nm on singular substrates to 800 and 500 nm on [100]- and [110]-miscut surfaces, respectively. In addition, Adams and Yalisove²⁵ reported a decrease in t_{epi} for Si on the higher index, and hence rougher (113), (115), and (117) surfaces compared to the (001) during MBE experiments on patterned Si substrates.

The results in Fig. 3 show that β_{eff} begins to increase rapidly with $t > 1 \mu\text{m}$ on the singular surface. Although it was not possible to obtain additional data at higher film thicknesses since $t_{\text{epi}} \approx 1200 \text{ nm}$,²⁰ repeated growth experi-

ments at the lower- t values were found to give the same results. The sudden increase in β_{eff} as t approached t_{epi} was predicted by Das Sarma *et al.*¹⁰ using a stochastic ballistic deposition model which includes adatom diffusion. In their model, the increase in β_{eff} was associated with a sudden onset of defect formation prior to the termination of epitaxial growth and the formation of an amorphous phase.

IV. CONCLUSIONS

In summary, our results show that low-temperature Si epitaxy is unstable on both singular and vicinal surfaces and leads to the development of well-defined growth mounds which coarsen with increasing film thickness. The growth surfaces are not self-affine, and the evolution of surface roughness is inconsistent with conventional scaling laws for kinetic roughening. The most important finding of this research, however, is that contrary to results obtained for high-temperature epitaxy in the step-flow regime, the Si(001) growth surface is more unstable on vicinal than on singular substrate surfaces during growth in the 2D multilayer mode.

ACKNOWLEDGMENTS

The authors gratefully acknowledge the financial support of the Joint Services Electronics Program, the Semiconductor Research Corporation, the U.S. Department of Energy through the University of Illinois MRL, and the Petroleum Research Fund. We also thank Professor A. Gewirth and Dr. M. Sardela for use of the AFM instrument and for x-ray-diffraction measurements, respectively.

-
- ¹J. Krug and H. Spohn, in *Solids Far From the Equilibrium*, edited by C. Grodèche (Cambridge University Press, Cambridge, England, 1991), p. 479; T. Vicsek, *Fractal Growth Phenomena* (World Scientific, Singapore, 1991), p. 386.
- ²F. Family, *Physica A* **168**, 561 (1990).
- ³J. Lapujoulade, *Surf. Sci. Rep.* **20**, 191 (1994).
- ⁴J. Villain, *J. Phys. I* **1**, 19 (1991).
- ⁵D. E. Wolf and J. Villain, *Europhys. Lett.* **13**, 389 (1990); M. Schroeder, M. Siegert, D. E. Wolf, J. D. Shore, and M. Plischke, *ibid.* **24**, 563 (1993).
- ⁶J. Krug, M. Plischke, and M. Siegert, *Phys. Rev. Lett.* **70**, 3271 (1993).
- ⁷M. D. Johnson, C. Orme, A. W. Hunt, D. Graff, J. Sudijino, L. M. Sander, and B. G. Orr, *Phys. Rev. Lett.* **72**, 116 (1994).
- ⁸M. Kotrla and P. Šmilauer, *Acta Phys. Slovaca* **44**, 237 (1994).
- ⁹M. Siegert and M. Plischke, *Phys. Rev. Lett.* **73**, 1517 (1994).
- ¹⁰S. Das Sarma, C. J. Lanczycki, S. V. Ghaisas, and J. M. Kim, *Phys. Rev. B* **49**, 10 693 (1994).
- ¹¹G. Ehrlich and F. Hudda, *J. Chem. Phys.* **44**, 1039 (1966).
- ¹²S. C. Wang and G. Erlich, *Phys. Rev. Lett.* **67**, 2509 (1991); **70**, 41 (1993); **71**, 4174 (1993).
- ¹³Y.-W. Mo and M. G. Lagally, *Surf. Sci.* **248**, 313 (1991); Y.-W. Mo, J. Kleiner, M. B. Webb, and M. G. Lagally, *ibid.* **268**, 275 (1992).
- ¹⁴Z. Zhang, Y.-T. Lu, and H. Metiu, *Phys. Rev. B* **46**, 1917 (1992).
- ¹⁵C. Roland and G. H. Gilmer, *Phys. Rev. B* **46**, 13 437 (1992); *Phys. Rev. Lett.* **67**, 3188 (1991).
- ¹⁶D. Srivastava and B. J. Garrison, *Phys. Rev. B* **47**, 4464 (1993).
- ¹⁷H.-J. Ernst, F. Fabre, R. Folkerts, and J. Lapujoulade, *Phys. Rev. Lett.* **72**, 112 (1994).
- ¹⁸J. E. Van Nostrand, S. J. Chey, M.-A. Hasan, D. G. Cahill, and J. E. Greene, *Phys. Rev. Lett.* **74**, 1127 (1995).
- ¹⁹J. Tersoff, A. W. Denier van der Gon, and R. M. Tromp, *Phys. Rev. Lett.* **72**, 266 (1994).
- ²⁰N.-E. Lee, G. A. Tomasch, and J. E. Greene, *Appl. Phys. Lett.* **65**, 3236 (1994).
- ²¹N.-E. Lee, G. A. Tomasch, G. Xue, L. C. Markert, and J. E. Greene, *Appl. Phys. Lett.* **64**, 1398 (1994).
- ²²H.-N. Yang, G.-C. Wang, and T.-M. Lu, *Diffraction From Rough Surfaces and Dynamic Growth Fronts* (World Scientific, Singapore, 1993), p. 136.
- ²³The effects of using a finite tip radius can be estimated based upon a model developed by J. E. Griffith and D. A. Grigg, *J. Appl. Phys.* **74**, R83 (1993). Assuming the worst case in our experiments with a 40-nm tip radius results in $[G(\rho, t)]^{1/2}$ being underestimated by 20% for films with mound separations $d < 20$ and 10% for films with larger mound separations. These uncertainties, which are inherent in the AFM measurements, were included in determining the overall uncertainties quoted in the text for the effective roughening and growth exponents α_{eff} and β_{eff} .
- ²⁴H.-N. Yang, G.-C. Wang, and T.-M. Lu, *Phys. Rev. Lett.* **73**, 2348 (1994).
- ²⁵D. P. Adams and S. M. Yalisove, *J. Appl. Phys.* **76**, 5185 (1994).